Peculiarities of deformation and destruction of porous titanium nickelide alloys at stretching, compression and bending

E. S. Marchenko, *Doctor of Physical and Mathematical Sciences, Associate Professor, Head of the Laboratory of Medical Alloys and Shape Memory Implants[1], e-mail: 89138641814@mail.ru*
G. A. Baigonakova, *Candidate of Physical and Mathematical Sciences, Assistant, Senior Researcher[1], e-mail: gat27@mail.ru*
A. S. Garin, *Post-Graduate Student, Research Engineer[1], e-mail: stik-020@mail.ru*
Yu. F. Yasenchuk, *Candidate of Physical and Mathematical Sciences, Associate Professor, Senior Researcher[1], e-mail: yayuri2008@gmail.com*

[1]*National Research Tomsk State University, Tomsk, Russia.*

The analysis of experimental data obtained during quasi-static tension, compression and bending of anisotropic and structurally inhomogeneous porous titanium nickelide alloys obtained by the method of self-propagating high-temperature synthesis (SHS) is carried out. It is shown that the studied porous titanium nickelide alloy near room temperature is in a pre-martensitic state and experiences a reversible martensitic transformation (MT) under the action of an external load. The influence of geometric anisotropy on the deformation behavior under tension and bending is shown. By means of quasi-static tension and three-point bending to failure of lamellar samples of porous titanium nickelide with a porosity of 60–70%, it was shown for the first time that all obtained strain curves are qualitatively self-similar and contain a basic block of two linear hardening sections and a yield section between them. It is shown for the first time that a decrease in the effective cross section and a decrease in the degree of geometric anisotropy of the deformation zone lead to the appearance of an additional yield region on the deformation curves of quasi-static tension. This indicates a significant dependence of the contribution of reversible martensitic deformation to the total deformation on the geometric anisotropy of porous titanium nickelide. An analysis of fracture surfaces showed the effect of the type and rate of loading on the ratio of brittle martensitic and ductile austenite phases in a multiphase matrix of a porous titanium nickelide alloy.

Key words: titanium nickelide, high-temperature synthesis, deformation, martensitic transformation, superelasticity, shape memory effect.

DOI: 10.17580/nfm.2022.02.12

Introduction

Among a large number of methods for studying the deformation behavior of structurally inhomogeneous alloys, the several effective methods can be identified, that are suitable for studying porous alloys with polymorphic phase transformation. Of these, the simplest, but quite effective method for studying the superelastic state of an alloy is uniaxial stretching [1–3]. The condition of this technique is the uniformity of the sample deformation, which is achieved by reducing its cross-section to a minimum size.

Since the precision grips are not used on most stretching machines, the experimental results obtained for stretching porous samples usually differ in the values of the maximum accumulated deformation and the destruction nature. When stretching porous titanium nickelide samples using precision grips, it is possible to achieve a relative elongation of 1–2%. In this case, the stretching curves are more informative and contain the accumulation areas of shear martensitic deformation. Besides, the uniformity of the stress state under uniaxial tension significantly depends on the geometric anisotropy of porous sample. The degree of geometric anisotropy increases with an increase of the sample's cross-section and the number of connections between the nodes of porous frame.

Due to the methodological difficulties of tensile testing, the deformation behavior of porous samples is more often investigated by the compression or torsion methods [4–11]. At that, it is easier to prepare samples for testing, and the requirements for the isotropy of equiaxial samples are not as high as at stretching plates. Therefore, the compression tests are much easier to carry out. However, in an equiaxially porous sample, the number of connections between the nodes is significantly greater than in a flat porous plate, and this feature imposes the significant restrictions on the manifestation of the superelastic properties of porous alloy. Due to such restrictions, the compression curves are significantly less informative for studying the superelastic behavior than the stretching curves.

Materials and methods

The deformation behavior of the SHS–TiNi was studied by single compression, stretching and bending to the destruction at room temperature on an testing machine INSTRON 3369. For compression testing by the electroerosion cutting methods, the samples with the dimensions of 3×3×6 mm were obtained. To study the influence of the dimensional factor on the features of the deformation behavior of SHS–TiNi alloys, the tests were carried out by uniaxial stretching of plates to rupture on a testing machine with a stretching speed of 1 mm/min. For the tensile tests, the samples were cut out in sizes 20×12×0.5; 20×12×3 and 20×12×6 mm. For bending tests up the fracture, the samples were obtained with dimensions 30×10×5; 30×10×3 and 30×10×0.5 mm, which were tested by the three-point bending method up the destruction. The samples were loaded at a rate of 0.3 mm/min.

Results and discussion

The stressed state analysis of the porous titanium nickelide samples should be carried out taking into account the geometric anisotropy of porous frame. Estimating the load distribution in the samples with an open porosity of 60–70%, they should be considered as a variety of rod structure in which the nodes' mobility is limited by the bridges' connections. The internal stresses in the volumetric undeformed porous frame are balanced, and the nodes and rods are in a tied state. The stresses developed in the frame's walls can lead to the destruction of the individual walls, but cannot lead to deformation of the entire volumetric frame. Therefore, the further mechanical tests were carried out on the samples from the porous alloys of different sizes.

At the quasi-static uniaxial compression before the destruction of the porous titanium nickelide samples with dimensions of 12×6×6 mm and 6×3×3 mm, the deformative dependences were obtained (**Fig. 1**) and the elastic limits and compressive strengths were determined (**Table 1**). There are no the yield areas on the dependencies, caused by stresses and associated with MT. Both curves are similar and have a form typical for an elastic-viscous deformation with hardening. The "steps" during the destruction indicate the brittle destruction of the bridges of porous frame.

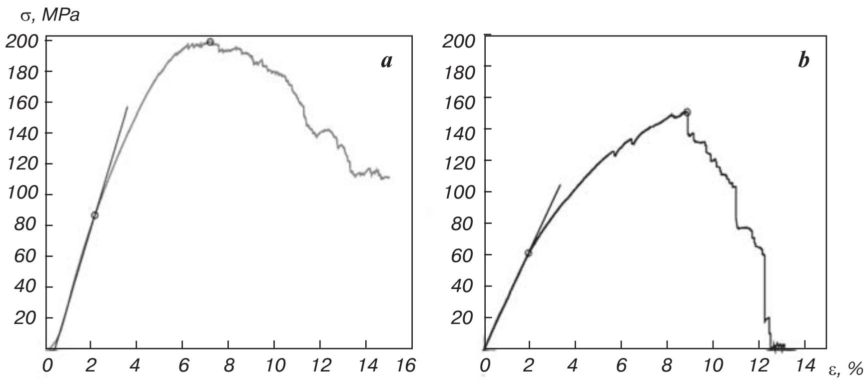

Fig. 1. Typical deformation diagrams obtained by uniaxial quasi-static compression of SHS-alloys of porous titanium nickelide:
a – 12×6×6 mm; *b* – 6×3×3 mm

At single compression up to the destruction of massive samples of 12×6×6 mm, an elastic section with an elastic limit of about 90 MPa was found on the deformation curve, under a relative narrowing of 2.2 %. The maximum compression stress was 197 MPa at the deformation of 7.1 % (**Table 1**).

At decreasing the cross-sectional dimensions of the samples from 6×6 to 3×3 mm, the number of bridges and the effective cross-sectional area of the sample decrease, at that the ultimate strength also decreases, and the curve's character saves (**Fig. 1, *b***).

Based on a series of experimental data, the assumption has been assumed that a high degree of geometric anisotropy of the porous framework in massive samples limits the inelastic martensitic deformation of titanium nickelide. Besides that, the irreversible plastic crumpling of porous frame occurs at compression. The obtained dependences make it possible to obtain only a macroscopic characteristic of a massive sample, not allowing to evaluate the inelastic martensitic behavior of the porous titanium nickelide alloy.

The dependences obtained by stretching thinner plates (thickness 3 and 0.5 mm) are more informative and have more characteristic areas of yield, associated with MT B2 → B19′, than the dependences obtained at destruction of plates with a thickness of 6 mm (**Fig. 2**). At decreasing the plates' thickness, the degree of geometric anisotropy decreases, at that the yield areas and areas of deformation hardening appear on the deformation curves (**Table 2**).

At stretching a porous plate with a size of 20×12×6 mm, the deformation curve, typical for the elastic-plastic materials, is obtained (**Fig. 2, *a***). The destruction surface

Table 1
Mechanical properties of porous titanium nickelide alloys obtained by single compression

Samples' sizes, mm	σ_y, MPa	σ_{comp}, MPa	*E*, GPa	ε_{el}, %	ε_{pl}, %	ε_{dest}, %
12×6×6	88.2 ± 6	197 ± 20	4.1 ± 0.3	2.2 ± 0.2	4.9 ± 0.4	7.1 ± 0.5
6×3×3	61.8 ± 5	153 ± 16	3.2 ± 0.1	1.9 ± 0.1	7.2 ± 0.6	9.1 ± 0.8

Remarks: σ_y – the elastic limit, σ_{comp} – the compressive strength, *E* – the elastic modulus, ε_{el} – the elastic deformation, ε_{pl} – the plastic deformation, ε_{dest} – the total deformation up to destruction.

Table 2
Mechanical properties of porous titanium nickelide alloys obtained by the SHS-method under stretching

Samples' sizes, mm	σ_m, MPa	σ_u, MPa	E, GPa	ε_{el}, %	ε_m, %	ε_{pl}, %	ε_{dest}, %
20×12×6	38.2 ± 3	114 ± 9	17.4 ± 1.3	0.3 ± 0.05	–	2.9 ± 0.2	3.2 ± 0.3
20×12×3	30.9 ± 2	167 ± 8	17.1 ± 1.1	0.2 ± 0.05	1.1 ±0.1	3.4 ± 0.3	4.7 ± 0.3
20×12×0.5	30.9 ± 2	101 ± 11	14.7 ± 1.5	0.2 ± 0.05	1.0 ± 0.1	1.1 ± 0.4	2.3 ± 0.3

Remarks: σ_m – the stress of martensitic shear; σ_u – the ultimate strength at stretching; E – the elasticity modulus on the section *A–B*; ε_{el} – the elastic deformation; ε_m – the martensitic deformation; ε_{pl} – the plastic deformation; ε_{dest} – the total deformation up to destruction.

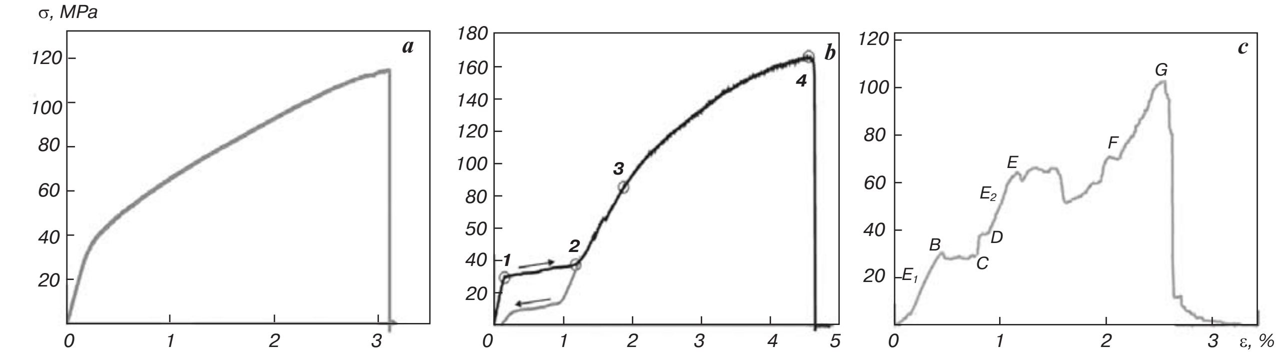

Fig. 2. Typical deformation diagrams, obtained by uniaxial stretching of porous plates of titanium nickelide: a – 20×12×6 mm; *b* – 20×12×3 mm; *c* – 20×12×0.5 mm

of a porous plate with a thickness of 6 mm contains from 400 to 500 bridges, which are oriented randomly relative to the load's direction. Due to this orientation, the bridges make a chaotic contribution to the general picture of deformation [12]. The greater the degree of anisotropy of porous framework and the more bridges are located in the destruction zone, the smaller the contribution of martensitic deformation to the additive deformation. Therefore, on the deformation dependence of massive plate are fewer peculiarities, associated with the martensitic deformation of the separate deformation cells.

The deformational dependence, obtained by stretching a porous plate with a size of 20×12×3 mm, is more informative, and it contains the elastic, martensitic and plastic areas of deformation (**Fig. 2, *b***). At the initial area of loading, all components of a multiphase porous alloy are deformed elastically. The portion *0–1* corresponds to the initial elastic deformation of the austenitic phase TiNi(B2). At the point *1*, corresponding to the yield strength of the alloy, the martensitic shear's stress is reached and begins MT TiNi(B2) → TiNi(B19′). The yield section on the portion *1–2* is caused by the phase transition TiNi(B2) → TiNi(B19′). The elastic portion *2–3* corresponds to the elastic deformation of the martensitic phase TiNi(B19′). Then, they are followed the nonlinear portion *3–4* of deformational hardening of the plastic deformation of the residual phase of TiNi(B2) and the porous frame. At the ultimate strength is reached at the point *4*, the brittle destruction of the martensitic phase TiNi(B19′) takes place [12–14]. At the selected cross-sectional dimensions of 12×3 mm, 300–370 bridges of the porous frame fell into the destruction zone of the samples. Thanks to the increase in the mobility of the porous frame, on the portion *1–2* of the deformation curve, the martensitic deformation features appeared of against the background of an additive deformation picture. At the unloading stage, at a relative deformation of 0.8 % the inelastic martensitic deformation is completely reversible, and the stress hysteresis $\Delta\sigma$ was 17 MPa, which is typical for the superelastic alloys. The area of the hysteresis loop corresponds to the dissipative losses, connected with an internal friction at the interphase boundaries at the reversible MT [15, 16].

At the thickness 0.5 mm of the porous plates, thanks to the maximum possible increase in the mobility of a single-layer porous frame, two self-similar blocks with a yield portion have already appeared on the deformation curve (**Fig. 2, *c***), which reflect the martensitic deformation's processes of the individual bridges in the porous frame. The self-similar sections differ in the magnitude of the maximum accumulated deformation and developed forces. The yield sites *M* correspond to the phase transition of austenite to martensite and further successive the brittle destruction of the porous frame's bridges. The so-called "yield tooth" is present at the boundaries of all fragments of the martensitic deformation. The magnitudes of the developed efforts of all fragments are comparable. A greater number of peculiarities on the deformational curve appeared thanks to a smaller number of ties (20–100 pcs.) between nodes in the destruction zone of the porous frame and thanks to an increase in their mobility (**Fig. 2**). The search and counting of bridges were carried out visually with the help of optical microscopy using the "focus stacking" technique and raster electron microscopy. From 30 to 80 images were used to obtain a single image on OM-microscopy (**Fig. 3**).

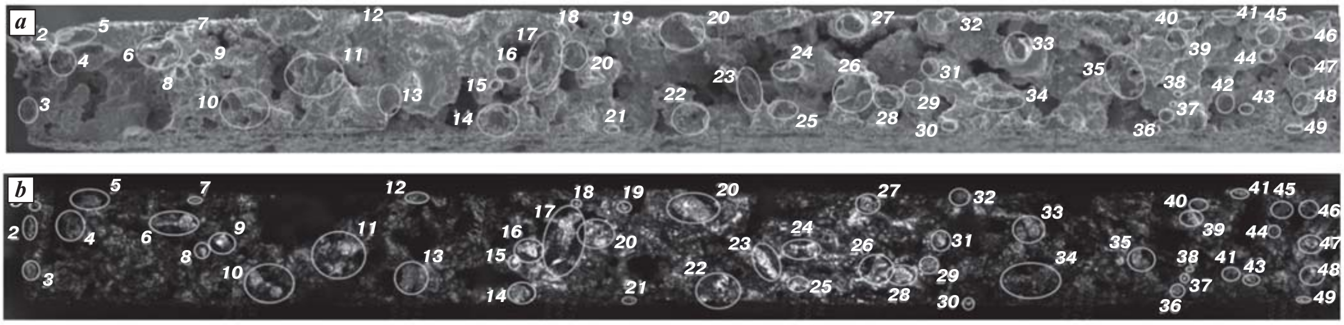

Fig. 3. Images of the fracture surface's fragment of the porous plate SHS–TiNi:
a – scanning electron microscopy; *b* – optical microscopy

Table 3
Mechanical properties of porous titanium nickelide alloys obtained by the SHS method at bending

Samples' sizes, mm	σ_m, MPa	σ_{bend}, MPa	*E*, GPa	ε_{el}, %	ε_m, %	ε_{pl}, %	ε_{dest}, %
30×10×5	54.9 ± 5	99 ± 8	4.2 ± 0.3	1.3 ± 0.1	–	1.9 ±0.2	3.2 ± 0.3
30×10×3	29.2 ± 4	113 ± 11	11.5 ± 1.2	0.2 ± 0.1	2.1 ± 0.3	0.9 ± 0.1	3.2 ± 0.3
30×10×0.5	11.8 ± 1	111 ±14	4.7 ± 0.3	0.3± 0.1	2.3 ± 0.2	1.7 ± 0.1	4.3 ± 0.4

Remarks: σ_m — the stress of martensitic shear; σ_{bend} — the ultimate strength at bending; *E* – the elasticity modulus on the section *A–B;* ε_{el} — the elastic deformation; ε_m — the martensitic deformation; ε_{pl} — the plastic deformation; ε_{dest} — the total deformation up to destruction

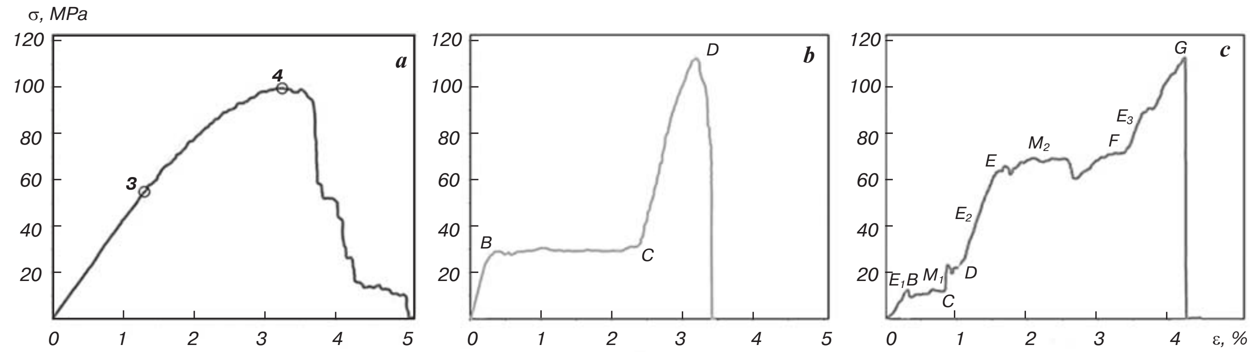

Fig. 4. Typical deformational diagrams obtained by three–point bending of porous plates from titanium nickelide:
a — 30×10×5 mm; *b* — 30×10×3 mm; *c* — 30×10×0.5 mm

Thus, a comparison of the stretching curves allows us to conclude that the size of the porous samples' cross–section and the anisotropy degree of the porous frame of the SHS-TiNi alloy significantly affect the number of self-similar blocks of the *ABCD* type of stretching curves (**Fig. 2, *b***).

The porous samples in the form of plates of the same porous TiNi alloy, which was tested by stretching, with dimensions 30×10×5; 30×10×3 and 30×10×0.5 mm have been tested by the three-point bending method up to destruction (**Fig. 4**, **Table 3**). As at stretching, the curves of three types were obtained, the appearance of which changed when the samples' sizes changed.

As at stretching, the curves obtained by bending the thickest samples do not have a yield portion. At bending samples with an average thickness of 3 mm, a curve from one block was obtained, which consists of a yield portion of about 2% in length, enclosed between two elastic hardening portions *E*1, *E*2. At bending a sample with the minimum thickness 0.5 mm, the curve from two blocks is obtained, which consist of a yield portion enclosed between two elastic hardening portions. The curves with the yield portions *M* correspond to brittle destruction of the bridges after a sequential phase transition of austenite to martensite in one or more bridges of the porous frame (**Fig. 4**, **Table 3**) [12, 13]. At that, the number of bonds in the destruction zone of plates with sizes of 300×100×0.5 mm did not exceed 60 pieces.

On the basis of the obtained data complex, it can be affirmed that during stretching and bending the qualitatively similar deformation curves have been obtained. The qualitative differences in curves within the same test method are caused by a significant quantitative difference in the effective cross-section and the number of bridges in the destruction zone of the porous frame.

Conclusions

It is established that the main distinguishing feature of the experimental deformation dependences, obtained by quasi-static compression, stretching and bending of samples of porous titanium nickelide, is the number and extent of the yield areas caused by martensitic transformation.

The main factor, influencing on the number and extent of yield areas during fracture by bending and stretching, is the geometric anisotropy of porous alloy. It is established that with uniaxial stretching of porous plates, characterized by minimal geometric anisotropy and having from 20 to 100 walls in the fracture zone of the porous frame, the destruction of the sample is achieved after passing two yield sections. The samples with a number of bridges up to 300 have one yield area on the deformation diagram due to martensitic transformation. An increase of the geometric anisotropy in porous frame with a number of bridges in the fracture zone of more than 400 leads to the regular disappearance of yield areas on the deformation curves.

Acknowledgments

The research was carried out with financial support of the Russian Science Foundation under the Grant No. 22-72-10037, https://rscf.ru/project/22-72-10037/.

References

1. Shariat B. S., Liu Y., Rio G. Pseudoelastic Behaviour of Perforated NiTi Shape Memory Plates under Tension. *Intermetallics*. 2014. Vol. 50. pp. 59–64.

2. Melton K. N., Mercier O. The Mechanical Properties of NiTi-Based Shape Memory Alloys. *Acta Metallurgica*. 1981. Vol. 29, Iss. 2. pp. 393–398.

3. Shinkin V. N. Direct and Inverse Non-Linear Approximation of Hardening Zone of Steel. *Chernye Metally*. 2019. No. 3. pp. 32–37.

4. Peng W., Liu K., Shah B. A., Yuan B., Gao Y., Zhu M. Enhanced Internal Friction and Specific Strength of Porous TiNi Shape Memory Alloy Composite by the Synergistic Effect of Pore and Ti2Ni. *Journal of Alloys and Compounds*. 2020. Vol. 816. 152578.

5. Resnina N., Belyaev S., Voronkov A., Gracheva A. Mechanical Behaviour and Functional Properties of Porous Ti-45 at.% Ni Alloy Produced by Self-Propagating High-Temperature Synthesis. *Smart Materials and Structures*. 2016. Vol. 25, Iss. 5. 055018.

6. Yang B., Luo Z., Yuan B., Liu J., Gao Y. High Damping of Lightweight TiNi-Ti2Ni Shape Memory Composites for Wide Temperature Range Usage. *Journal of Materials Engineering Performance*. 2017. Vol. 26, Iss. 10. pp. 4970–4976.

7. Resnina N., Belyaev S. P., Voronkov A. Functional Properties of Porous Ti-48.0 at. % Ni Shape Memory Alloy Produced by Self-Propagating High Temperature Synthesis. *Journal of Materials Engineering and Performance*. 2018. Vol. 27, No. 3. pp. 1257–1264.

8. Zhang L., Zhang Y. Q., Jiang Y. H., Zhou R. Superelastic Behaviors of Biomedical Porous NiTi Alloy with High Porosity and Large Pore Size Prepared by Spark Plasma Sintering. *Journal of Alloys and Compounds*. 2015. Vol. 644. pp. 513–522.

9. Li B. Q., Wang C. Y., Lu X. Effect of Pore Structure on the Compressive Property of Porous Ti Produced by Powder Metallurgy Technique. *Materials and Design*. 2013. Vol. 50. pp. 613–619.

10. Otsuka K., Ren X. Physical Metallurgy of Ti-Ni-Based Shape Memory Alloys. *Progress Materials Science*. 2005. Vol. 50, No. 5. pp. 511–678.

11. Shinkin V. N. Springback Coefficient of Round Steel Beam Under Elastoplastic Torsion. *CIS Iron and Steel Review*. 2018. Vol. 15. pp. 23–27. DOI: 10.17580/cisisr.2018.01.05

12. Marchenko E. S., Yasenchuk Yu. F., Gunter S. V. et al. Viscoelastic Behavior of Biocompatible Titanium Nickelide Alloys. Tomsk: Tomsk State University, 2020. 102 p.

13. Yasenchuk Yu. F., Marchenko E. S., Baigonakova G. A. et al. Study on Tensile, Bending, Fatigue, and in vivo Behavior of Porous SHS-TiNi Alloy Used as a Bone Substitute. *Biomedical Materials*. 2021. Vol. 16, Iss. 2. 021001.

14. Marchenko E. S., Baigonakova G. A., Gunther V. E. Effect of Alloying of Titanium Nickelide-Based Alloys with Group V Elements (Vanadium, Niobium) on Their Mechanical Properties. *Russian Metallurgy (Metally)*. 2018. No. 10. pp. 990–994.

15. Kornilov I. I., Belousov O. K., Kachur E. V. Titanium Nickelide and Other Alloys with the Effect of "Memory". Moscow: Nauka, 1977. 179 p.

16. Marchenko E. S., Baigonakova G. A., Gunter V. E., Klopotov A. A. Martensitic Transformations in Alloys Based on Titanium Nickelide with Silver Additives. *Novye Materialy i Tekhnologii*. Barnaul: Altai State University, 2017. pp. 54–57. NFM